

LARGE INHOMOGENEOUS ROADWAY DEFORMATION MECHANISM AND CONTROL UNDER MINING EFFECTS

Wang, Z. G.^{*,**,#}; Yin, S. L.^{*}; Wang, X. Q.^{*}; Sun, T.^{*} & Fan, M. Y.^{*}

^{*} College of Energy and Mining Engineering, Xi'an University of Science and Technology, Xi'an, 710054, China

^{**} Key Laboratory of Western Mine Exploitation and Hazard Prevention Ministry of Education, Xi'an University of Science and Technology, Xi'an, 710054, China

E-Mail: zhigangwong@xust.edu.cn (# Corresponding author)

Abstract

To reveal the mechanism of large inhomogeneous roadway deformation under mining effects and realize effective control, this study employed multiple research methods to analyse the evolution laws of the stress environment and plastic zones of the 5105 roadway in service under the engineering background of the gob-side entry in Selian No. 1 Coal Mine, China. The mechanism of the large inhomogeneous deformation of the mining roadway was revealed, and a full-section differentiated control technique was proposed. Results demonstrate that the roadway at 5 m in front of the working face is under a stress environment, in which the principal stress ratio is 3.77 and the included angle between the maximum principal stress and the horizontal direction is 64°. This stress state induces inhomogeneous malignant extension in the plastic zone in the roof at the coal-rib side and in the floor at the coal-pillar side. A full-section differentiated control technique involving roof and rib reinforcement with asymmetric bolt/cable support and floor pressure relief by hole drilling and cable bolting was developed. Numerical simulation revealed the technique's good control effect.

(Received in March 2026, accepted in April 2026. This paper was with the authors 2 weeks for 1 revision.)

Key Words: Gob-Side Entry, Inhomogeneous Deformation, Numerical Simulation, Plastic Zone, Surrounding Rock Control

1. INTRODUCTION

As an important part of the global energy structure, coal resources play an important role in the global economy [1, 2]. Underground longwall mining, one of the main mining methods, involves the layout of mining roadways, which serve as the "throat" of longwall mining systems, and its stability control has always been a key technical difficulty restricting the safe, efficient production of mines [3-5]. For roadways located in zones superposed with the advanced mining stress of the working face and the lateral abutment pressure from the adjacent goaf, the surrounding rock is subject to an extremely complicated coupling stress field and usually presents intense inhomogeneous deformation, which is typically characterized by the local subsidence of the roof, the differentiated extrusion of two ribs, and the asymmetric heaving of the floor. This type of uncoordinated deformation can impede the normal advancement of the working face and lead to dynamic disasters, including roof caving and rib instability-induced heaving [6, 7]. The large inhomogeneous deformation mechanism of gob-side entries under mining effects needs to be explored to ensure that roadways are safe and reliable throughout the service period, and scientific, reasonable control measures must be proposed.

In existing studies, abutment pressure theory [8, 9] was applied to explain the stress environment of surrounding rock of roadways. Such an analytical approach based on the increase in stress magnitude struggles to explain the asymmetric and directional deformation characteristics of surrounding rock. According to butterfly-shaped plastic zone theory developed in recent years [10, 11], the morphology of the surrounding rock's plastic zone depends on the principal stress and is controlled by the ratio and direction of this stress.

Therefore, when analysing the surrounding rock stress environment of mining roadways, emphasis should be placed on the spatiotemporal evolution of the stress vector. Given the insufficient understanding of the abovementioned mechanism, the traditional idea of left–right symmetry and uniform layout [12, 13] has been mostly followed in mainstream practice when designing the roadway support mode under mining effects. The surrounding rock of the mining roadway presents inhomogeneous, asymmetric failure modes. In this case, the persistent use of symmetric support parameters can lead to support resource wastage on the non-key stress-bearing side and induce structural instability because of the insufficient support strength in key failure zones.

Against the engineering background of a gob-side entry in Selian No. 1 Coal Mine, China, this study integrates field investigation, theoretical analysis, and numerical simulation methods to analyse the surrounding rock stress evolution of the roadway at advanced positions of the working face and the distribution characteristics of plastic zones. The internal mechanical mechanism of large inhomogeneous roadway deformation under mining effects is revealed, and surrounding rock control measures and a support optimization scheme are proposed for the roadway to provide a new idea for recognizing the large inhomogeneous roadway deformation mechanism under mining effects and achieving stability control.

2. RELATED WORKS

The instability mechanism of this kind of surrounding rock of mining roadways has been extensively investigated through theoretical analyses, numerical simulations, and field measurements, and useful results have been obtained.

For instance, Xu et al. [14] comprehensively analysed the stress state and deformation law of a fully mechanized caving roadway and concluded that the inhomogeneous stress field induced by intense mining is the main cause of asymmetric deformation. Wu et al. [15] analysed the multiple superposition effects of lateral abutment pressure of the goaf, mining stress in the upper coal seam, and advanced mining stress of the roadway. The research showed that this multisource stress superposition is the root cause of the substantial regional asymmetric failure of surrounding rock. Li et al. [16] comprehensively conducted field monitoring, numerical simulation, and theoretical analysis and concluded that regional high-stress rotation is the root cause of asymmetric roadway failure. Shan et al. [17] analysed the spatial distribution characteristics of deviatoric stress and plastic zones and found that the increase in the stress concentration coefficient of surrounding rock and the deflection of the maximum principal stress direction jointly induce asymmetric roadway deformation. In the studies above, the primary emphasis was on static analysis of the distribution state and directional deflection of the stress fields of surrounding rock and their effects on the stability of surrounding rock from a macro perspective. For roadways subject to the strong superposition of lateral stress from the adjacent goaf and advanced mining stress of the working face, with the advancement of the working face, the surrounding rock experiences a complicated, dynamic evolution process of sustained changes in the magnitude and direction of its principal stress. In existing research, the spatiotemporal evolution characteristics of the principal stress vector field in this process were not quantitatively characterized. So the disaster-causing effect under the coupled action of the superposed high principal stress at specific positions and the deflection of the principal stress remains unclear.

Considering the poor control effect of surrounding rock in mining roadways and the difficulty of disaster prevention and control, some scholars have proposed control techniques. Jin et al. [13] developed a reasonable roof control scheme for a mining roadway via FLAC3D software by applying the support mode of four columns for one beam within the 20 m range in front of the working face of the transportation roadway, which is intensely affected, with an

array pitch of 0.8 m; they achieved a good field application effect. Klishin et al. [18] presented a movable roof support for coal mine roadways, determined the characteristics of the failure zone and the effect of the support on the surrounding rock, and provided the application scope of this support in mine roadways. To address the roadway instability problem under adverse geological conditions, Jilo et al. [19] evaluated the effectiveness of the support system via numerical simulations and reported that roadway deformation can be effectively relieved through the anchor bolt–shotcrete combined support technique. Wang et al. [20] proposed a roof and rib control method applicable to the differentiated support of the soft intercalated layer in the advanced composite roof through high-strength, thick anchoring, which can realize continuous stress transfer and geometrically coordinated deformation. Eremin and Peryshkin [21] concluded that the initial well spacing influences the crack formation time and the spatial distribution of damage accumulation zones, and the hydrofracturing technique can effectively reduce the abutment pressure of the working face. Qian et al. [22] studied the stability of surrounding rock in an advanced mining roadway on a deep working face, proposed a long anchorage–roof-cutting blasting–stress relief combined control technique, and verified its feasibility through engineering practice. The core control strategies in the abovementioned studies mainly focus on the roof and ribs, mostly adopting the traditional symmetric support mode. Although differentiated control has been applied in some studies, the important role played by the floor in the overall stability of surrounding rock has frequently been neglected. Under this unbalanced control concepts, the roadway can become prone to the structurally imbalanced state of poor adaptation of roof and rib support to asymmetric deformation and absence of floor control when faced with the composite working conditions of advanced superposed stresses and soft floors, thus inducing overall instability.

Given the limitations of existing studies, this study adopted a gob-side entry in Selian No. 1 Coal Mine, China, as the study object. Field investigation, theoretical analysis, and numerical simulation methods were combined to systematically explain the large inhomogeneous deformation of the gob-side entry under the mining effect, and a full-section differentiated control technique was established. It provides a new idea for elucidating the mechanism of the large inhomogeneous deformation of mining roadways and achieving stability control.

The remainder of this study is organized as follows. Section 3 presents the engineering background, modelling, and simulation scheme. Section 4 analyses the stress and plastic zone distribution in the surrounding rock of the roadway, reveals the large inhomogeneous deformation mechanism of the mining roadway, and introduces relevant control measures and the proposed support scheme. Section 5 provides the conclusions.

3. METHODOLOGY

3.1 Engineering background

In Selian No. 1 Coal Mine, China, the 4-1 coal seam is mainly mined at present. It has an average vertical depth of 220 m, coal thickness of 2.35–5.19 m, average coal thickness of 4 m, and a dip angle of 0°–2°, and it belongs to a nearly horizontal and medium-thickness coal seam with a simple occurrence structure. The borehole column diagram of the working face is displayed in Fig. 1 a.

The study object is the 5105 roadway in the 4-1 coal seam. The sectional dimensions of this roadway are 5,100 × 3,850 mm (width × height). Tunnelling was performed along the floor of the coal seam, with a 20 m coal pillar away from the goaf of the adjacent 8107 working face, and the specific position layout relation is shown in Fig. 1 b.

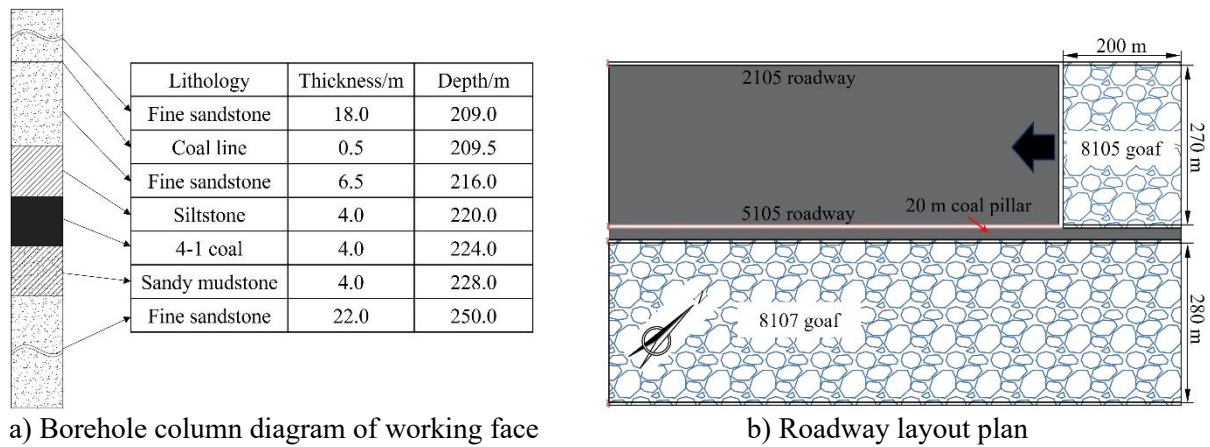


Figure 1: Diagram of borehole of the working face and roadway layout.

The bolt–mesh + W-shaped steel strips + single prop support were adopted for the roadway within the advanced section of this working face. The support parameters are as follows:

(1) Roof support: $\Phi 20 \times 2,400$ mm left-handed threaded steel bolts without longitudinal reinforcement were used, with 6 in each row, at a spacing and row distance of $900 \times 1,000$ mm. $\Phi 17.8 \times 7,200$ mm prestressed strands were adopted as cables, with 3 in each row, at a spacing and row distance of $1,350 \times 2,000$ mm. Moreover, $4,800 \times 275 \times 3$ mm W-shaped steel strips were applied, with 6 holes in each block and a hole spacing of 900 mm.

(2) Rib support: $\Phi 20 \times 2,400$ mm glass fibre-reinforced plastic bolts were used on the coal-rib side, with 3 in each row, at a spacing and row distance of $1,200 \times 1,000$ mm. $\Phi 20 \times 2,400$ mm left-handed threaded steel bolts without longitudinal reinforcement were applied on the coal pillar ribs, with 3 in each row, at a spacing and row distance of $1,200 \times 1,000$ mm.

(3) Floor and advanced support: C30 concrete with a thickness of 300 mm was poured on the floor. The advanced support distance was 25 m, and DW40-250/110XL (G) single hydraulic props with π -shaped steel beams were used in the support zone, with 4 in each row, at a spacing and row distance of $1,000 \times 1,000$ mm.

Roadway deformation failure characteristics under the mining effect: The 5105 roadway in the advanced support zone of the 8105 working face presented obvious local inhomogeneous, asymmetric deformation, which was mainly manifested as follows: (1) the rock on the roof on the coal-rib side was severely broken; (2) the rock at the top of the coal rib was severely broken, but the bottom integrity was good; (3) the rock at the top of the coal-pillar side was broken, and the bottom heaved obviously up to 300 mm; and (4) the floor heaved unevenly (the floor heave was much greater on the coal-pillar side than on the coal-rib side), and the maximum heaving amount could reach 400 mm. The deformation and failure of the roadway are shown in Fig. 2.

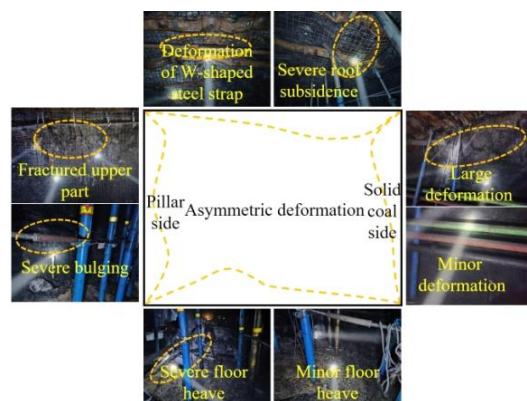


Figure 2: Real photo of the asymmetric failure site of the 5105 roadway.

3.2 Establishment of the numerical model

A numerical model (Fig. 3) was built with FLAC3D6.0 to reveal the large inhomogeneous deformation and failure mechanism of surrounding rock of the roadway under the mining effect. The model had dimensions of 610 m × 600 m × 100 m (length × width × height). A total of 4,199,280 meshes were generated, and the number of nodes was 4,452,037. Displacement constraints were applied to the front, back, left, right, and lower boundaries of the model. Stress constraints were imposed on the upper boundary, and 4.30 MPa of vertical stress was applied to the top of the model in accordance with the geostress data. The lateral pressure coefficient was set to 1.49, and the Mohr–Coulomb criterion was adopted. The mechanical properties of each rock stratum in the model are listed in Table I.

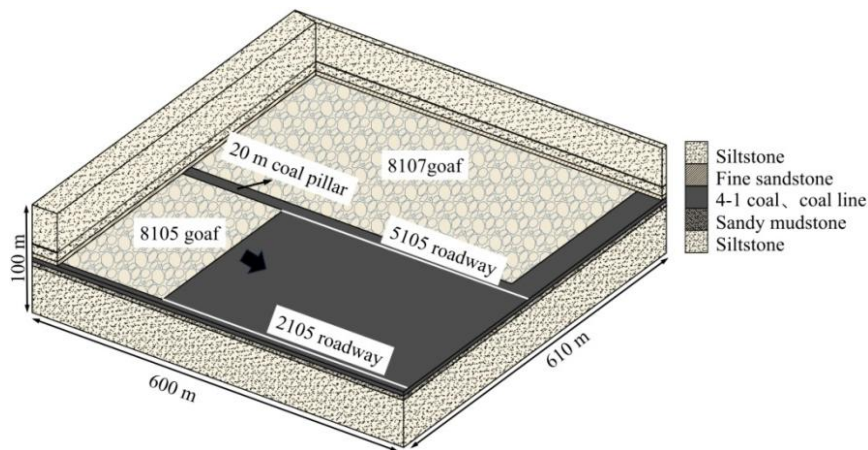


Figure 3: Numerical calculation model.

Table I: Mechanical parameters of the model.

Lithology	Density (kg·m ⁻³)	Bulk modulus (GPa)	Shear modulus (GPa)	Friction angle (°)	Cohesion (MPa)	Tensile strength (MPa)
Siltstone	1937	2.04	1.34	32	1.65	1.5
Coal line	1390	1.67	0.77	27	1.35	0.5
Siltstone	1937	2.04	1.34	32	1.65	1.5
Fine sandstone	2064	3.51	2.52	35	3.20	2.54
4-1 coal	1390	1.67	0.77	27	1.35	0.5
Sandy mudstone	2212	2.05	1.05	28	2.00	1.7
Siltstone	1961	2.03	1.27	30	1.60	1.4

3.3 Simulation analysis scheme

To obtain the stress state and plastic zone distribution characteristics of the surrounding rock of the roadway with different distances ahead of the working face, on the basis of the actual working conditions of the 5105 roadway, the model calculated the mining of the 8107 working face, followed by the mining of the 8105 working face. The focus was on analysing the changes in the roadway stress field characteristics and plastic zones at different distances ahead of the working face.

The goaf was filled using a double-yield model to equivalently simulate the compaction characteristics of the caving body in the goaf and improve the model's computational accuracy. The double-yield compression simulation experiment was continuously implemented through the trial-and-error inversion method [23, 24]. The physical and mechanical parameters of rocks in the caving zone obtained through the inversion are listed in Table II.

Table II: Physical and mechanical parameters of the caving zone.

Property	Density ($\text{kg}\cdot\text{m}^{-3}$)	Bulk modulus (GPa)	Shear modulus (GPa)	Friction angle ($^{\circ}$)	Cohesion (MPa)	Dilation angle ($^{\circ}$)
Value	1700	12.5	5.6	10	0.001	8

4. ANALYSIS OF RESULTS

4.1 Analysis of regional stress field characteristics of the roadway

The lateral principal stress distribution after mining of the 8107 working face is shown in Fig. 4 a. The lateral principal stress within a specific distance changed substantially because of the mining of the adjacent working face. The principal stress value increased and then declined, and the principal stress ratio gradually decreased. The maximum principal stress gradually contra-rotated from the deviation to the coal-rib side to the vertical direction; subsequently, it continued to rotate toward the horizontal direction. The maximum principal stress at the centre of the 5105 roadway was 9.63 MPa, the minimum principal stress was 6.86 MPa, the principal stress ratio was 1.40, and the included angle between the direction of the maximum principal stress and the horizontal direction was 30.17° .

As the working face advanced to 100 m, the distribution of the principal stress at the centre of the roadway ahead of the 8105 working face is shown in Fig. 4 b. The magnitude of the principal stress exhibited a trend of initially increase and then decline; the ratio of principal stresses continuously diminished; and the direction of the maximum principal stress gradually rotated from an angle of 76.8° with horizontal to approximately 30° .

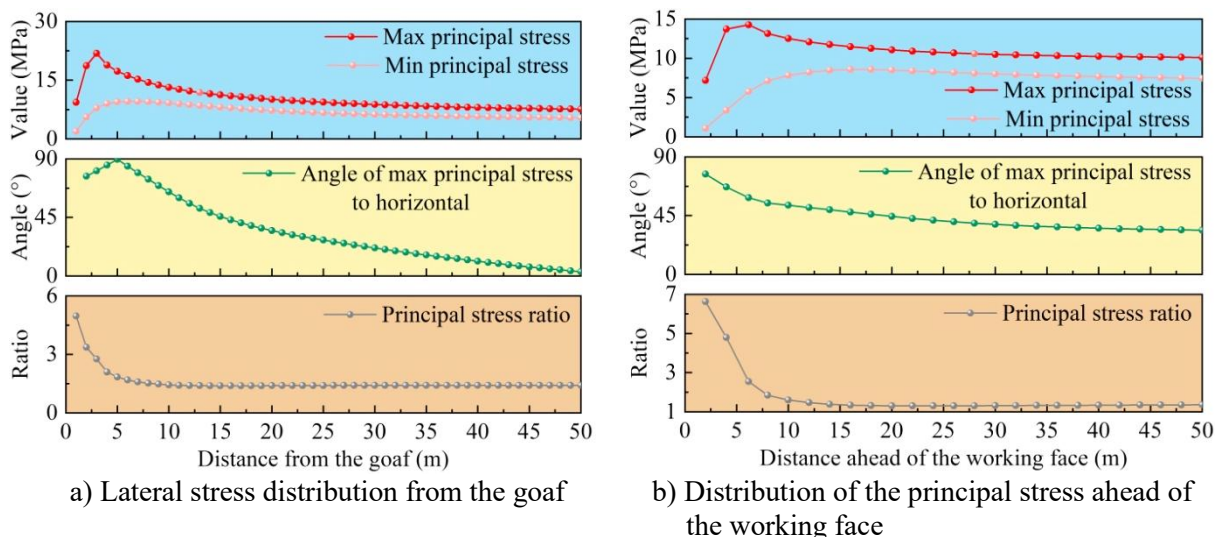


Figure 4: Distribution characteristics of principal stresses lateral to the goaf and ahead of the working face.

The analysis above indicates that under the advanced mining effect of the adjacent goaf and working face, the stress of the surrounding rock of the roadway is in a high-deviatoric-stress field, where the peak value of the principal stress is high and the stress direction

deflects. Under such a stress field, the plastic failure characteristics of the roadway are different from those in the stable tunnelling period.

4.2 Large inhomogeneous deformation mechanism of surrounding rock of the roadway

On the basis of the previous analysis of the stress distribution, the deformation and failure results of the surrounding rock upon the advancement of the working face by 100 m were acquired, as shown in Fig. 5.

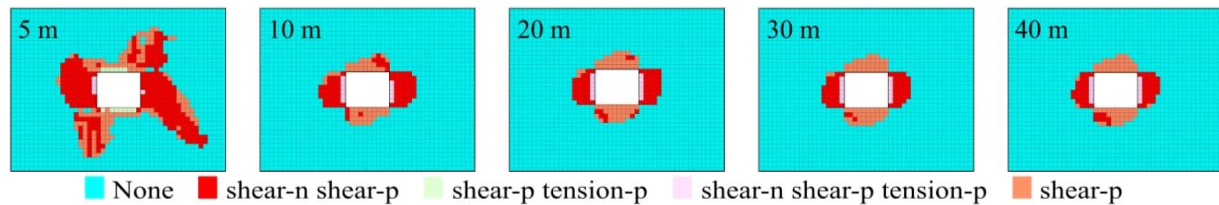


Figure 5: Plastic zone distribution characteristics at advanced positions.

Fig. 5 indicates that at the position of 5 m ahead of the working face, under the disturbance superposed by the advanced mining stress and lateral stress, the plastic zones of the surrounding rock of the 5105 roadway exhibited a notable asymmetric butterfly-shaped malignant extension form. With the deflection of the principal stress, the butterfly-shaped plastic zones developed deeply toward the roof at the coal-rib side and the floor at the coal-pillar side. This extension form coincided with the field-observed deformation part of the surrounding rock in the advanced intense failure zone of the working face. As the distance from the working face increased (from 5 m to 40 m), the mining stress continued to decline. Within the advancement interval of 10 m to 20 m, the peak deviatoric stress of the surrounding rock decreased, the butterfly-leaf deflection in the plastic zone underwent rapid degeneration and shrinkage, and the failure depth substantially decreased; when the advancement distance exceeded 20 m, the stress environment of the surrounding rock of the roadway gradually stabilized. In this case, the roadway was only affected by the 8107 goaf, the morphology of the plastic zone became approximately elliptical, and the range of development was kept constant.

On the basis of the analysis results of the stress state and distribution characteristics of the plastic zones, the mechanism of inhomogeneous large deformation of the roadway under the influence of mining can be summarized as follows: because of the double disturbance created by the 8107 goaf and the 8105 working face, the 5105 roadway was in the coupled stress field of the superposition of residual abutment pressure from the adjacent goaf and advanced mining of this working face. When the 8105 working face advanced to 100 m, the principal stress ratio of the roadway at the position of 5 m ahead reached 3.77, and the direction of the maximum principal stress deflected at an angle of about 64° with the horizontal direction. The plastic zone of the roadway surrounding rock expanded in a nonuniform butterfly shape under the influence of this highly deviant stress field, thus inducing nonuniform large deformation of the roadway surrounding rock.

4.3 Roadway control measures under the mining effect

According to the analysis above, the plastic zone of the surrounding rock of the 5105 roadway presented typical butterfly-shaped inhomogeneous malignant extension characteristics. Such inhomogeneous plastic failure characteristics led to the intense asymmetry of roadway deformation. Hence, whether the directional malignant extension of butterfly-shaped plastic zones can be effectively inhibited is the key to ensuring the long-term stability of surrounding rock in similar roadways.

According to literature [10, 11], a roadway is susceptible to butterfly-shaped failure under a high-deviatoric-stress environment, and reasonable control measures in terms of stress control in this case should include adjusting regional stress fields by optimizing the coal mining sequence, reasonably arranging the roadway position, and drilling advanced pressure relief holes that can improve the malignant morphology of plastic zones of the roadway. As revealed in literature [11, 20], directional deflection of principal stress in the regional high-deviatoric-stress environment triggers a deflectional butterfly form of plastic zones of the roadway, and differentiated loosening forms are manifested at shallow parts of surrounding rock with weak load-bearing capacity. In this case, if the support resistance provided by the composite load-bearing structure composed of bolts/cables at shallow parts is high enough, the residual strength of broken rock mass can be effectively enhanced, forming a large-scale effective compressive stress zone that can markedly reduce the extension rate of plastic zones. However, the homogeneous symmetric layout is mostly adopted in traditional roadway support, but it cannot match the asymmetric, inhomogeneous failure characteristics of such mining roadways with poor adaptability to local positions with severe plastic failures. This situation aggravates the hidden risk of local roof caving and intense side-rib heaving. Therefore, a reasonable layout of bolts/cables should consider the failure depth and position of surrounding rock, and differentiated support methods should be adopted to balance and inhibit large inhomogeneous deformation.

According to the analysis above, control measures specific to the large inhomogeneous, butterfly-shaped deformation failure of the mining roadway should adopt the following ideas:

(1) Active pressure relief to improve the regional stress environment: During the mining period of the working face, weakening or fracture zones can be proactively fabricated in the high-stress-concentration zone of surrounding rock of the roadway through manual intervention techniques, such as deep hole presplitting blasting and floor drilling pressure relief. Doing this can improve the stress state of the surrounding rock and constrain the evolutionary trend of the plastic zones from an elliptic shape to the malignant butterfly shape.

(2) Reinforcement and support in local zones sensitive to plastic failure: The conventional homogeneous, symmetric support mode neglects the difference in the failure depth of plastic zones at different parts. In this case, the zones susceptible to plastic failure in the roof and rib can be identified in accordance with the butterfly-shaped distribution laws of plastic zones revealed in the numerical simulation, together with the parts with the hidden risk of large deformation as observed on site. Pertinent reinforcement measures (e.g., increasing the anchorage depth of cables, densifying asymmetric rib support, and applying a high prestress) should be implemented for such zones so that the support strength can match the potential energy of inhomogeneous deformation of the surrounding rock, thereby reducing the risk of local roof caving and large asymmetric deformation of the roadway.

4.4 Stability support design of the 5105 roadway

On the basis of the surrounding rock control measures for the roadway and by combining the failure modes of surrounding rock of the 5105 roadway, a combined support scheme of roof and rib reinforcement with asymmetric bolt/cable support and pressure relief by floor hole drilling + cable bolting was designed for this roadway, as shown in Fig. 6.

Local reinforcement support technique for the roof and rib: The design adopted bolt/cable-reinforced support to replace single hydraulic props, and local zones with a large range of plastic failure on the roof and rib are subject to densified reinforcement support as follows: 4 roof cables were applied on each row, with an optimized row spacing of 1,000 mm, and a $\Phi 17.8 \times 7,200$ mm cable was added on the roof at 300 mm from the coal-rib side, forming an included angle of 30° with the vertical direction; a $\Phi 20 \times 2,400$ mm glass fibre-reinforced plastic bolt was added on the coal rib at 700, 1,100, and 2,100 mm from the top,

1,500 mm from the coal-pillar side. A marked asymmetric extrusion form was presented on the two ribs. The optimization scheme displacement is shown in Fig. 7 b. The maximum displacement of the roof and floor is 119.49 and 110 mm, respectively. While substantially improving the stability of surrounding rock, this optimization scheme radically releases the space occupied by single props, thereby solving the narrow space and operating difficulty induced by the large number of props under the traditional support mode.

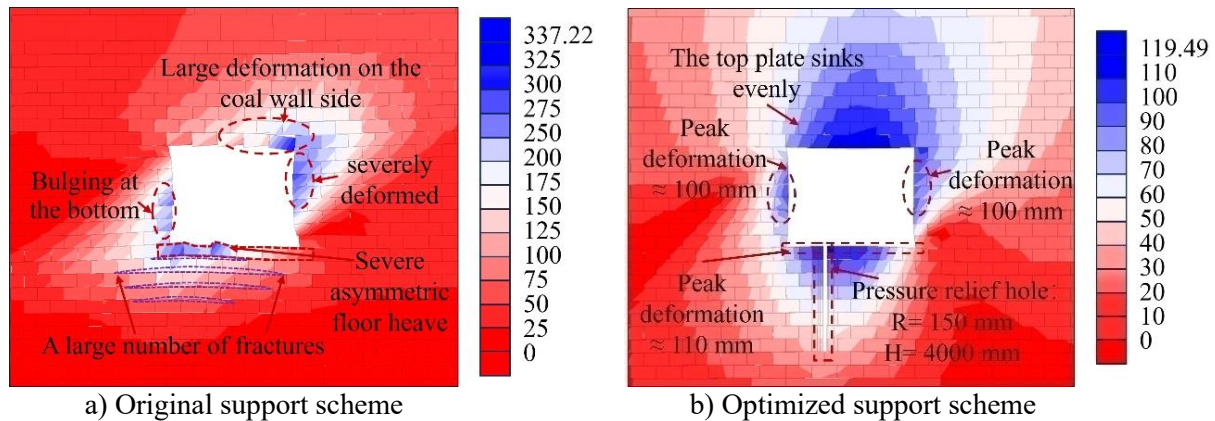


Figure 7: Overall displacement cloud maps of the roadway under original and optimized support schemes (mm).

5. CONCLUSIONS

To reveal the large inhomogeneous roadway deformation mechanism under the mining effect and realize roadway stability control, this study acquired the regional stress field characteristics and the distribution laws of plastic zones of the roadway under the mining effect through numerical calculations on the basis of field investigation. Then, the large inhomogeneous roadway deformation mechanism was determined, and a differentiated combined support technique was proposed. The following conclusions were obtained.

(1) As the distance from this working face increases, the regional maximum principal stress initially increases and then decreases, the principal stress ratio rapidly declines until it reaches stability, and the stress gradually rotates from the approximately vertical direction to the coal-pillar side before stabilizing at an included angle of about 30° with the horizontal direction.

(2) Affected by the residual stress in the adjacent goaf and the advanced mining stress of this working face, the 5105 roadway 5 m ahead of this working face is in a high-deviatoric-stress environment, in which the extreme value of the principal stress ratio reaches 3.77 and the principal stress deflects. The plastic zones of the surrounding rock present a deflectional butterfly shape, which is the fundamental cause of the large inhomogeneous deformation of the surrounding rock.

(3) On the basis of the distribution form of the plastic zones of the surrounding rock of the 5105 roadway and its deformation characteristics, a full-section differentiated combined support technique of roof and rib reinforcement with asymmetric bolt/cable support and floor pressure relief by hole drilling + cable bolting was proposed and verified through numerical simulation. The method exerts a good control effect on the surrounding rock.

In brief, the stress field characteristics of the surrounding rock of the roadway under the mining effect and the distribution laws of plastic zones were systematically analysed in this study. The obtained morphologies of the plastic zones of the surrounding rock were in line with the field-observed deformation situation, verifying the reasonability of the proposed internal mechanism. However, only the numerical simulation method was adopted in this

study. In the future, the proposed technique can be further verified through field industrial tests to provide a solid engineering basis for the stability control of mining roadways.

ACKNOWLEDGEMENT

This work was supported by the National Natural Science Foundation of China (52204155).

REFERENCES

- [1] Jasansky, S.; Lieber, M.; Giljum, S.; Maus, V. (2023). An open database on global coal and metal mine production, *Scientific Data*, Vol. 10, Paper 52, 12 pages, doi:[10.1038/s41597-023-01965-y](https://doi.org/10.1038/s41597-023-01965-y)
- [2] Agrawal, R.; Ragauskas, A. J. (2025). Sustainable recovery of Rare Earth Elements (REEs) from coal and coal ash through urban mining: a Nature Based Solution (NBS) for circular economy, *Journal of Environmental Management*, Vol. 384, Paper 125411, 18 pages, doi:[10.1016/j.jenvman.2025.125411](https://doi.org/10.1016/j.jenvman.2025.125411)
- [3] Kang, H.; Gao, F.; Xu, G.; Ren, H. (2023). Mechanical behaviors of coal measures and ground control technologies for China's deep coal mines – a review, *Journal of Rock Mechanics and Geotechnical Engineering*, Vol. 15, No. 1, 37-65, doi:[10.1016/j.jrmge.2022.11.004](https://doi.org/10.1016/j.jrmge.2022.11.004)
- [4] Yetkin, M. E.; Ozfirat, M. K.; Onargan, T. (2024). Examining the optimum panel pillar dimension in longwall mining considering stress distribution, *Scientific Reports*, Vol. 14, Paper 6928, 12 pages, doi:[10.1038/s41598-024-57579-w](https://doi.org/10.1038/s41598-024-57579-w)
- [5] Han, U. C.; Choe, C. S.; Hong, K. U.; Pak, C. (2022). Prediction of final displacement of tunnels in time-dependent rock mass based on the nonequidistant grey Verhulst model, *Mathematical Problems in Engineering*, Vol. 2022, Paper 3241171, 11 pages, doi:[10.1155/2022/3241171](https://doi.org/10.1155/2022/3241171)
- [6] Li, J.; Ren, J.; Li, C.; Zhang, W.; Tong, F. (2023). Failure mechanism and stability control of soft roof in advance support section of mining face, *Minerals*, Vol. 13, No. 2, Paper 178, 17 pages, doi:[10.3390/min13020178](https://doi.org/10.3390/min13020178)
- [7] Chen, Y.; Zhang, S.; Wang, S. R.; Cao, Y. X.; Lutynski, M. (2025). Simulation analysis of creep evolution process in soft-hard composite coal seams, *International Journal of Simulation Modelling*, Vol. 24, No. 3, 485-496, doi:[10.2507/IJSIMM24-3-736](https://doi.org/10.2507/IJSIMM24-3-736)
- [8] Yadav, A. R.; Islavath, S. R. (2024). Numerical investigation for estimation of behaviour of barrier pillars, gateroads and face of a deep longwall mine: a case study, *Mining, Metallurgy & Exploration*, Vol. 41, No. 1, 463-478, doi:[10.1007/s42461-023-00891-2](https://doi.org/10.1007/s42461-023-00891-2)
- [9] Zhou, S.; Shi, H. (2024). Pressure evolution of overlying rock strata using gradual increase support mining method, *International Journal of Simulation Modelling*, Vol. 23, No. 2, 263-274, doi:[10.2507/IJSIMM23-2-683](https://doi.org/10.2507/IJSIMM23-2-683)
- [10] Han, Z.; Liu, H.; Guo, L.; Cheng, W.; Liang, J.; Chen, Z.; Guo, X.; Wang, H. (2025). A full-plane strain complex variable analytical model considering three-dimensional principal stress rotation and its engineering applications, *International Journal of Coal Science & Technology*, Vol. 12, No. 1, Paper 88, 18 pages, doi:[10.1007/s40789-025-00828-8](https://doi.org/10.1007/s40789-025-00828-8)
- [11] Shu, S.; Wang, W.; Ma, Y.; Yuan, C.; Tian, X.; Du, R.; Ge, S. (2026). Research on the evolution law of the plastic zone and control technologies for surrounding rock in floor roadway influenced by mining activities, *Energy Science & Engineering*, Vol. 14, No. 1, 444-459, doi:[10.1002/ese3.70366](https://doi.org/10.1002/ese3.70366)
- [12] Mesutoglu, M.; Ozkan, I. (2024). Evaluation and comparison of rock bolting versus steel arch support systems in thick coal seam underground galleries: a case study, *Mining, Metallurgy & Exploration*, Vol. 41, No. 4, 1719-1737, doi:[10.1007/s42461-024-00994-4](https://doi.org/10.1007/s42461-024-00994-4)
- [13] Jin, Z.; Xu, Y.; Peng, T.; Gao, L. (2021). Roof control technology of mining roadway under the influence of advanced supporting pressure, *Advances in Civil Engineering*, Vol. 2021, Paper 2049755, 8 pages, doi:[10.1155/2021/2049755](https://doi.org/10.1155/2021/2049755)
- [14] Xu, X.; He, F.; Li, X.; He, W. (2021). Research on mechanism and control of asymmetric deformation of gob side coal roadway with fully mechanized caving mining, *Engineering Failure Analysis*, Vol. 120, Paper 105097, 12 pages, doi:[10.1016/j.engfailanal.2020.105097](https://doi.org/10.1016/j.engfailanal.2020.105097)

- [15] Wu, P.; Liang, B.; Jin, J.; Li, G.; Wang, B.; Guo, B.; Yang, Z. (2022). Research of roadway deformation induced by mining disturbances and the use of subsection control technology, *Energy Science & Engineering*, Vol. 10, No. 4, 1030-1042, doi:[10.1002/ese3.1094](https://doi.org/10.1002/ese3.1094)
- [16] Li, C.; Wu, Z.; Zhang, W.; Sun, Y.; Zhu, C.; Zhang, X. (2020). A case study on asymmetric deformation mechanism of the reserved roadway under mining influences and its control techniques, *Geomechanics and Engineering*, Vol. 22, No. 5, 449-460, doi:[10.12989/GAE.2020.22.5.449](https://doi.org/10.12989/GAE.2020.22.5.449)
- [17] Shan, R.; Li, Z.; Wang, C.; Wei, Y.; Bai, Y.; Zhao, Y.; Tong, X. (2021). Research on the mechanism of asymmetric deformation and stability control of near-fault roadway under the influence of mining, *Engineering Failure Analysis*, Vol. 127, Paper 105492, 17 pages, doi:[10.1016/j.engfailanal.2021.105492](https://doi.org/10.1016/j.engfailanal.2021.105492)
- [18] Klishin, V. I.; Fryanov, V. N.; Pavlova, L. D.; Nikitenko, S. M.; Malakhov, Y. V. (2021). Rock mass-multifunction mobile roof support interaction in mining, *Journal of Mining Science*, Vol. 57, No. 3, 361-369, doi:[10.1134/S1062739121030017](https://doi.org/10.1134/S1062739121030017)
- [19] Jilo, N. Z.; Assefa, S. M.; Assefa, E. (2024). Numerical analysis of underground tunnel deformation: a case study of Midroc Lega-Dembi gold mine, *Scientific Reports*, Vol. 14, Paper 7964, 24 pages, doi:[10.1038/s41598-024-57621-x](https://doi.org/10.1038/s41598-024-57621-x)
- [20] Wang, P.; Zhang, N.; Kan, J.; Xu, X.; Cui, G. (2022). Instability mode and control technology of surrounding rock in composite roof coal roadway under multiple dynamic pressure disturbances, *Geofluids*, Vol. 2022, Paper 8694325, 19 pages, doi:[10.1155/2022/8694325](https://doi.org/10.1155/2022/8694325)
- [21] Eremin, M. O.; Peryshkin, A. Y. (2025). Analysis of the influence of the well spacing on the formation of an effective crack network in the hard-to-cave coal roof during hydraulic fracturing based on mathematical modeling, *Physical Mesomechanics*, Vol. 28, No. 3, 397-408, doi:[10.1134/S1029959924601477](https://doi.org/10.1134/S1029959924601477)
- [22] Qian, D.; Deng, J.; Wang, S.; Yang, X.; Cui, Q.; Li, Z.; Jin, S.; Liu, W. (2022). Deformation characteristics and control countermeasures for surrounding rock of deep roadway under mining disturbance: a case study, *Shock and Vibration*, Vol. 2022, No. 1, Paper 9878557, 12 pages, doi:[10.1155/2022/9878557](https://doi.org/10.1155/2022/9878557)
- [23] Yavuz, H. (2004). An estimation method for cover pressure re-establishment distance and pressure distribution in the goaf of longwall coal mines, *International Journal of Rock Mechanics and Mining Sciences*, Vol. 41, No. 2, 193-205, doi:[10.1016/S1365-1609\(03\)00082-0](https://doi.org/10.1016/S1365-1609(03)00082-0)
- [24] Chen, D.; Wang, X.; Wu, S.; Zhang, F.; Fan, Z.; Wang, X.; Li, M. (2023). Study on stability mechanism and control techniques of surrounding rock in gob-side entry retaining with flexible formwork concrete wall, *Journal of Central South University*, Vol. 30, No. 9, 2966-2982, doi:[10.1007/s11771-023-5436-z](https://doi.org/10.1007/s11771-023-5436-z)